Microfabrication by a High Fluence Femtosecond Exposure: Mechanism and Applications

Mitsuru Watanabe,[a] Saulius Juodkazis,[a] Junji Nishii,[b] Shigeki Matsuo,[a] and Hiroaki Misawa[a]

[a]Department of Ecosystem Engineering, The University of Tokushima,
2-1 Minamijyosanjima, Tokushima 770-8506, Japan
[b]AIST Kansai, Ikeda, Osaka 563-8577, Japan

ABSTRACT

We report the observation of 3/2-frequency generation during an Optically-induced failure of silica under femtosecond laser pulse irradiation. The origin of 3/2-frequency generation is due to a two-plasmon decay instability, which occurs at the quarter critical density of free charge carriers. We observed this emission during the optical damaging of glasses by tightly focused (numerical aperture of the objective lens was 0.5-1.35) femtosecond laser pulses. The pulse duration at the irradiation spot was about 0.35 ps, the energy 25-250 nJ, and the damage was recorded in a single shot event inside the glass. The emission at about 530 nm was only present in the spectra measured during an optical damage by 795 nm irradiation with the pulse energy 9 times and more higher than the threshold.
We observed a new phenomenon applicable for microstructuring of glass. The high energy fs pulses (50-200 μJ) were focused by a plano-convex lens (focal length 2-10 cm) on the exit surface of a glass plate. The surface was ablated and the ablation was transferred into a volume of glass by translation of a "plasma spark". The length of such a channels can by up to few-cm and with a diameter of tens-of-micrometers. The mechanism and application of high-fluence fs fabrication in dielectrics is discussed.

Keywords: direct laser writing, dielectric breakdown, two plasmon decay instability, silica, light-induced damage threshold, microfabrication

1. INTRODUCTION

Microstructuring and microfabrication of materials by ultra-short 100-400 fs (1 fs = 10^{-15} s) pulses find new fields of application, especially, where three-dimensional (3D) freedom of fabrication inside transparent solid[1] or liquid[2] material is necessary. At the same time, a full understanding of laser light-material interaction is still missing in the case of fs exposure. 3D microstructuring is elucidated even less than the ablation due to an inherent difficulty to apply such techniques as mass spectrometry and time-of-flight methods, which have been proven to be essential in the ablation studies.

Light induced damage threshold (LIDT) for a 3D microstructuring is usually defined as the light intensity (or fluence) necessary to generate critical density of electrons, N_{cr}.[3] The maximum free charge carriers concentration to be reached by optical excitation is defined by the plasmon frequency as $\omega_{pl} = \sqrt{4\pi N_{cr} e^2/(m_e m^*)}$, where e is the electron charge, m^* and m_e are the gravity and effective mass of electron, respectively. When plasmon frequency is equal to that of laser irradiation, the material reflects the laser light (the reflection coefficient $R \to 1$). This is true for the ideal case of homogeneous plasma and at right angle incidence. However, in the case on non-homogeneous plasma and in the presence of longitudinal light field along its propagation, as it is in the case of oblique incidence of p-polarization (or at tight focusing), the light energy can be further delivered to the plasma region. In fact, namely this principle is used in experiments on laser induced nuclear fusion experiments where longitudinal energy transfer from light to matter is implemented.

Definition of LIDT via N_{cr}, however, does not describe the nature of the phenomenon of *dielectric (optical) breakdown*, which is a total photoionization of focal volume via non-linear absorption processes. Technically LIDT can be defined as the intensity/fluence at which residual structural modifications of material is introduced. Obviously, this criterion of LIDT determination is dependent on the measurement technique used to examine the modification.

Author information for correspondence:
S.J.: E-mail address: saulius@eco.tokushima-u.ac.jp.
H.M.: Corresponding author. E-mail address: misawa@eco.tokushima-u.ac.jp. (fax: (+81) 88 656 7598)

Photon Processing in Microelectronics and Photonics, Koji Sugioka, Malcolm C. Gower,
Richard F. Haglund, Jr., Alberto Piqué, Frank Träger, Jan J. Dubowski, Willem Hoving, Editors,
Proceedings of SPIE Vol. 4637 (2002) © 2002 SPIE · 0277-786X/02/$15.00

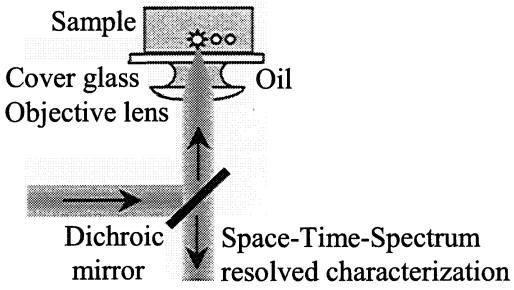

Figure 1. Principal setup of fabrication and characterization using a high numerical aperture, $NA > 1$, objective lens.

Here we describe an experiment aimed at fs microstructuring by fluencies corresponding to free carrier densities lower than N_{cr}. We examined a light emission from the irradiation spot during dielectric breakdown for a characterization of the breakdown. Also, the fabrication by a plasma spark scanned inside the glass is demonstrated. This technique allowed microstructuring on a mm-to-cm length scale.

2. EXPERIMENTAL

Fs-fabrication was carried out by amplified 150 fs pulses obtained from laser setup, which consists of Ti:sapphire *Tsunami* oscillator and regenerative (chirped pulse) amplifier *Spitfire*, both from *Spectra Physics*. The output power was about 500 mW at 1 kHz repetition rate. This radiation was delivered to sample under fabrication by focusing with (i) plano-convex lens or (ii) microscope (Fig. 1). The pulse energy at irradiation point was calculated and is specified where it applies. For a optical damaging with two consecutive fs-pulses we used an Mach-Zehnder-type interferometer setup to split and to combine coaxially two fs-pulses of perpendicular polarizations.[4] Microstructuring of transparent dielectric materials by fs-pulses using simple plano-convex lens focusing requires typically $20-200$ μJ/pulse energies, while the microstructuring in the microscope needs just $10-100$ nJ/pulse. More details on the setup can be found elsewhere.[1] We used silica (purified to have OH and Cl contamination lower than 100 ppm) and borosilicate glass BK7 for our experiments.

Spectral characterization of light emission from the irradiation spot (Fig. 1) observed at fluencies below and above that of dielectric breakdown was carried out by *Oriel* spectrometer, which was set to a side port of a microscope. In such a geometry (Fig. 1), the window for spectral observation was limited by the transmission of a dichroic mirror in the microscope (spectral profile is given in Fig. 2). Structural modifications of exposed glass were tested by their response to wet etching in BHF (49%HF with 100%NH_4F) water solutions.

3. RESULTS AND DISCUSSION

In this section we will, first, explore the possibility of microstructuring of silica at the irradiation intensities, which correspond to a free carrier plasma density $N_{cr}/4$, second, we will compare surface ablation with 3D optical damaging by the fabricated damage sizes, and, third, we will introduce a novel mechanism of microstructuring of glass by an ablation front, which was scanned into the bulk of sample, the "plasma spark" method. Fabricated channels were characterized by optical cross-polarized imaging and wet etching.

3.1. Generation of 3/2-frequency during dielectric breakdown

In order to reduce cost of fs-fabrication the attempts are made to decrease the LIDT of fabrication by, either, modification of glass by the doping of absorptive agents[5] or by quasi-cw exposure to fs pulses as it was demonstrated in the case of a waveguide recording in silica. The motivation is to avoid the use of regenerative amplifier, which increases the cost and complexity of microfabrication setup. This prompted us to examine the possibility to microstructure glass by irradiation, which correspond to the free carrier plasma densities less than N_{cr}. If such a microstructuring would be possible, the measurement of light emission spectrum observed during dielectric breakdown (or at a fluence below it) is expected to be a good tool to evaluate the density of electrons in plasma. Indeed, the presence of, so called, $3/2\omega$ frequency should indicate the free carrier density of just $N_{cr}/4$.

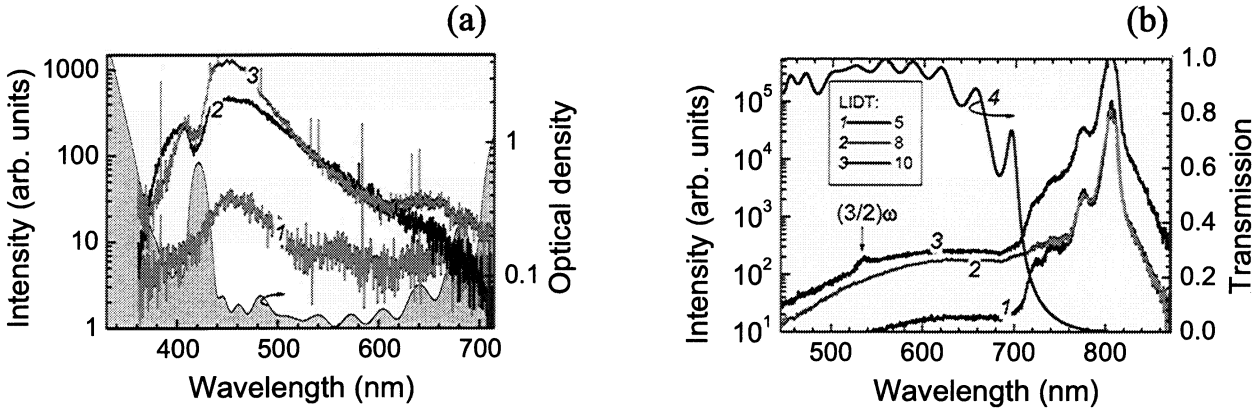

Figure 2. (a) Radiation spectra observed during an optical breakdown of silica by sub-ps pulses at different fluencies (background subtracted): by one pulse of $0.5LIDT$ (*1*), at damaging by the two pulses separated by 30 ps $LIDT(2) = 0.7 \times LIDT + 0.2 \times LIDT$ (*2*), and by one pulse at $1LIDT$ (*3*). The transmission spectrum of microscope is given by a gray profile (right axis). Optical damage was made inside silica, pulse duration at the irradiation point was 0.35 ps for one-pulse and 0.45 ps for two-pulses irradiation, the wavelength 795 nm.
(b) Spectra of light emission of optical breakdown from a focal point in silica at different fs-irradiation fluencies at 800 nm wavelength. The emission at $3/2\omega$ (around 530 nm) is shown by arrow. Spectral profile of registration path in microscope is given on the right axis.

Strictly speaking the light emission below and above LIDT should be distinguished. At lower fluencies, below the LIDT, the emission is called white light continuum (WLC) or super-continuum(ps[6,7]; fs[8,9]), while at a dielectric breakdown the emission is caused by thermal plasma radiation (PR). Phenomenon of WLC can occur in a wide variety of transparent condensed media[8,10] and in gases.[9] The general characteristics of the femtosecond continuum are as follows: its spectral width depends on the medium in which is generated,[11] its spectrum is modulated,[6] its polarization is in the same direction as the polarization of the input pulse,[11] and its anti-Stokes frequency components lag temporally its Stokes components.[8,12] The fs-continuum exhibits a smaller beam divergence than the ps-continuum.[9] It is found that its anomalous divergence does not imply the absence of strong self-focusing but is rather due to a self-guiding mechanism that involves the Kerr effect.

Especially intriguing is the mechanism that determines it's spectral width. Among the various mechanisms that have been suggested so far, we find self-phase modulation (SPM),[6,8,13] ionization-enhanced SPM,[14] and four-wave mixing.[6,15] It is at present generally believed that the main mechanism in fs-continuum generation is SPM enhanced by self-steepening of the pulse.[7,13] A shortcoming of this model is its prediction of a broader continuum in media with higher Kerr nonlinearity, a trend that is not observed[7] (the bandgap dependence dominates - large bandgap implies lower Kerr effect).

Experiments have shown that the power threshold for continuum generation coincides with the calculated critical power for self-focusing.[9,16] This is not surprising, considering that the onset of catastrophic self-focusing at critical power leads to a drastic increase in intensity, which can enhance SPM. This coincidence also suggests an intimate connection between the WLC and the mechanism that stops catastrophic self-focusing. Such a connection was first proposed by Bloembergen[14] to explain the ps-continuum. In his model, self-focusing is stopped by avalanche ionization; the appearance of free electrons enhances SPM and results in the continuum. A similar mechanism can be envisaged for fs-continuum generation in condensed media. In this case, an important mechanism of free-electron generation is multiphoton excitation (MPE).[17]

Figure 2 shows light emission collected from an irradiation spot inside silica at different fluencies (setup of experiment is given in Fig. 1). Transmission window of the microscope optics is given in (Fig. 2(a)) and, in fact, was limiting spectrally the emission, which was extending from UV-to-IR[18] under the direct measurement (not in microscope). An interesting result was that at the fluence of $0.5LIDT$ the emission band around 470 nm was present. However, at the lower fluencies no WLC emission was observed in one or two-pulse experiments (for a time

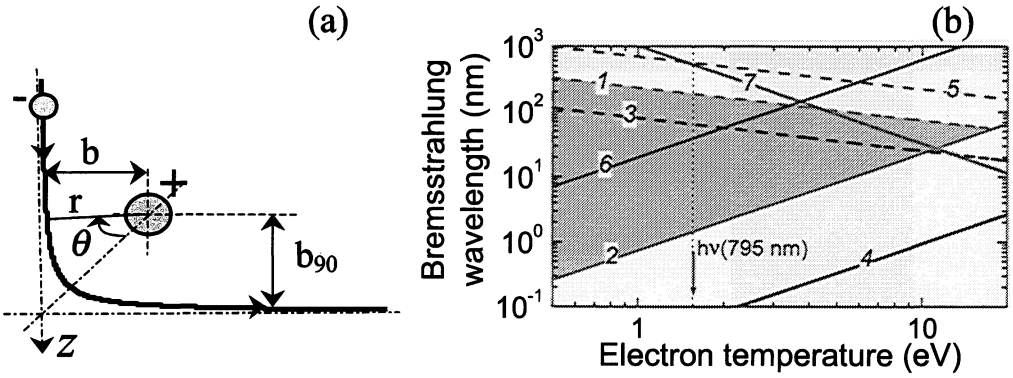

Figure 3. (a) Geometry of electron-ion collision. The impact distance is b, the right angle scattering length is b_{90}. (b) Approximate spectral extent of *bremsstrahlung* vs. free electron temperature for linear (*1, 3, 5*) and parabolic (*2, 4, 6*) electron-ion collisions. The impact distance expressed in Si-O bond length is: $b = 1$ (*1, 2*), 0.34 - (*3, 4*), and 3 - (*5, 6*). The line *7* marks the frequency where spectra due to linear collisions is overridden by that from parabolic ones. The gray region marks the main spectral content of radiation at impact distance $b = 1$.

separation between pulses 0-20 ps). This implies that microstructuring at fluencies, which correspond to a free carrier concentration (FCC) below N_{cr} is not possible.

Only at extremely high fluencies over $9LIDT$ we detected a weak emission of $(3/2)\omega$ (Fig. 2(b)). Spectra in Fig. 2(b) were numerically deconvoluted from the transmission profile of microscope transmission (curve *4*). This emission is a signature of parametric instability, known as 3/2-frequency generation or two-plasmon decay (TPD).[19] This laser plasma instability occurs at a quarter critical density $N = N_{ec}/4$, which corresponds to the plasma wave at a plasmon frequency, $\omega_p = \omega/2$, where ω is the cyclic frequency of laser irradiation. The impulse of the laser light scattered from such a plasma excitation, $\mathbf{k}_s$, can be matched by two plasma waves. As a result of impulse matching $\mathbf{k}_s = \mathbf{k}_p + \mathbf{k}_p$, the laser scattered light will possess the frequency component at $3\omega/2$. Also, the higher harmonic generation at half-harmonic frequencies $\omega = (n+1)\omega$ is expected; here n is the integer. It was demonstrated that $(3/2)\omega$ emission has a threshold at 1×10^{14} W/cm^2 in BK7 type glass (K8 in Russian nomenclature) and it depends on the driving pulse intensity, I_0, as $I_{(3/2)\omega} \propto I_0^{3/2} T_e^{3/2}$,[20] where T_e is the electron temperature in plasma. In our case the $3\omega/2$ emission corresponds to a 530 nm wavelength light, which was submerged into the broad emission band, the origin of which will be discussed bellow. Threshold intensity for $(3/2)\omega$ emission in silica we found at 1.6×10^{14} W/cm^2. It is worth to note that the 0.1 PW/cm^2 light intensity is corresponding to the electron quiver (oscillating) energy of 6 eV for a linear polarization at 0.8 μm wavelength according to the following scaling dependence[21]:

$$E_{osc}[\mathrm{eV}] = 9.3(1+\alpha^2)\frac{I}{10^{14}[\mathrm{W/cm^2}]}(\lambda[\mu\mathrm{m}])^2 \qquad (1)$$

where $\alpha = 1$ or 0 for the circular and linear polarizations, respectively. Threshold emission at $(3/2)\omega$ corresponds to a 9.6 eV quiver energy, which almost perfectly coincides with the bandgap of silica at 9-10 eV.

The possible explanation of spectrally broad radiation can be understood in the frame of a free moving electron in the Coulomb field of an ion, what is known as the *classical bremsstrahlung* (German word for "braking radiation"). This is the most probable source of light emission since there is a poor compliance of silica luminescence bands with experimentally observed spectra during optical damage. Spectrally broad XUV-to-infrared radiation is expected from a free electron passing the ion due to its "braking". The hyperbola path of free electron in spherical coordinates r, θ is given by formulas:[22]

$$r = \frac{b^2}{b_{90}(1+\epsilon\cos\theta)}; \quad b_{90} = \frac{Ze^2}{4\pi\varepsilon_0 m^* v^2}; \quad \epsilon = \sqrt{1+\left(\frac{b}{b_{90}}\right)^2}, \qquad (2)$$

where b is the impact distance, b_{90} is the distance at $\theta = -\pi/2$ scattering, v is the velocity of an electron, and ϵ is the eccentricity (Fig. 3(a)). The *bremsstrahlung* radiation is a direct consequence of an acceleration (or deceleration)

of charged particle; the radiated energy, W, per unit angular frequency is given by:[22]

$$\frac{dW}{d\omega} = \frac{e^2}{6\pi^2\varepsilon_0 c^3}\left|\int_{-\infty}^{\infty} \dot{v}e^{i\omega t}dt\right|^2, \tag{3}$$

where $\dot{v}$ is the acceleration of an electron. Spectral content of *bremsstrahlung* depends on the type of electron-ion collision. At first, let us consider free-free type encounters, where the incoming electron is not captured into an available electronic shell of an ion and is free after the collision. There are two types of collisions: the linear ones, when $b \ll b_{90}$ and the parabolic at $b \gg b_{90}$, here b_{90} is the electron-ion distance at right angle scattering. The short wavelength edge of spectra for these two types of collisions is plotted in Fig. 3(b) for the different impact distance b as a function of electron energy. The value of b is expressed in terms of Si-O bond length (1.62 Å) to evaluate the possible radiation spectrum in silica. The distance of 0.34×1.62 Å is, for example, the distance traveled by a free electron during the half of optical cycle at 795 nm wavelength (Fig. 3(b) lines *3,4*). The radiation spectrum at this value of b could be considered as a light-induced "friction" of an electron with the ion, from which the electron was freed. At large value of 3×1.62 Å the electron is moving in the field of an atom from the neighboring SiO_3 tetrahedron. Figure 3(b) qualitatively shows the extent of spectrum expected in the case of *bremsstrahlung*. As one can see the most blue-shifted spectrum is expected from parabolic collisions. The line *7* (Fig. 3(b)) demarks the spectrum caused by the linear collisions from that of parabolic ones and is given by v/b_{90}. At the electron energies larger than 1 eV the *bremsstrahlung* is expected to be caused mainly by parabolic electron-ion encounters due to the increased probability of inelastic scattering at the large electron energies.

The model of *bremsstrahlung* radiation qualitatively well explains the origin of continuum (in which part it is applicable to WLC and PR is still needs investigation). This is particularly appealing explanation for a continuum emission observed from the focal point of the size comparable with the wavelength, because in this case the length of light propagation in the photomodified region is extremely small, on the order of the Rayleigh distance, and there is no plausible explanation of spectral broadening due to the optical nonlinear effects (e. g. self-phase modulation (SPM) the longitudinal Kerr $\chi^{(3)}$ effect), which could explain a spectral broadening of spectrum up to UV region for the laser wavelength of 795 nm .

Light emission during optical breakdown has a number of components, which can be separated by their time decays and characteristic emission bands. For example, a shock-compressed lime-glass at 110 GPa has an emission peak at 490 nm, which corresponds to a 5700 K temperature.[23] One could expect a contribution of fractoluminescence (FL)[24,25] to a radiation spectrum of optical damage in silica. The emission band at 650 nm in Fig. 2(a) could be actually caused by the FL as it was observed in similar low-OH-content silica.[25] This band is attributable to a non-bridging oxygen hole center (NBOHC). Typical time scale of FL is from μs-to-ms. Finally, a photo-luminescence (PL) is always present in a recorded spectrum of optical damage and can be distinguished by the corresponding bands. Usually, a long lasting PL spectrum of glass is spectrally similar to a FL. Apart of FL, which occurs during the crack formation and propagation as a result of recombination of excited state of defects or atoms (ions, molecules), the sonoluminescence[26] (SL) is expected to occur as well. This is a "milder" response of material to the optically driven shock wave propagating in solid media. The cause of SL is the recombination of separated charges during dislocation movement. Similar mechanism is applicable to the amorphous material such as silica and is expected to occur during the dielectric breakdown induced by sub-ps pulses.[27] SL might originate on the extended area as compared with the size of focal point of irradiation. Spectral form-factors of SL and FL are similar, what is caused by their origin on the recombination of charges separated on the defect sites. Also, the spiking emission from the atomic, ionic, and molecular species are usually present.

3.2. Power dependence of laser ablation of silica

For a Gaussian pulse/beam the ablation threshold can be determined from the following dependence:

$$A_{th} = A_0 \exp(-(D/w)^2), \tag{4}$$

where D is the diameter of crater, w is the diameter of beam at $1/e$-level, and A_{th} with A_0 stands respectively for threshold and amplitude of the incident light expressed in terms of energy, fluence (energy density), or intensity. Figure 4 shows the data on laser ablation plotted along with predictions calculated by eqn. 4. The diameter of crater measured by atomic force microscopy (AFM) was found following eqn. 4 in terms of fluence (Fig. 4(b)) much better than in terms of pulse energy (Fig. 4(a)). It was found that surface ablation took also place at pulse energies

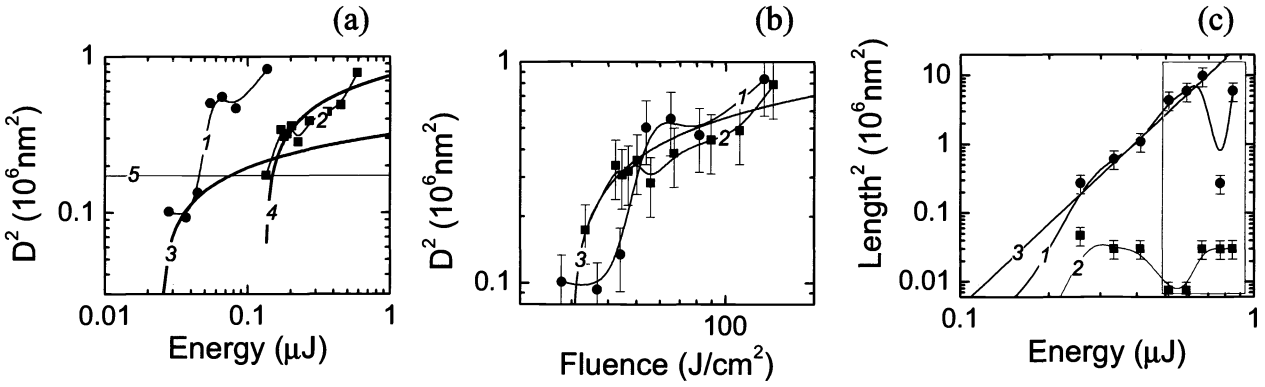

Figure 4. The dependence of the ablation crater diameter, D, on incident pulse energy (a) and fluence (b) for an ablation by a single pulse at $\lambda = 400$ nm (*1*) and at 800 nm (*2*). Curves *3* and *4* are plotted by eqn. 4 with $w = 1.1\lambda$. Curve *5* depicts an *in situ* observable LIDT in optical transmission microscope. Curve *3* in (b) was plotted by eqn. 4 with $w = 0.92\lambda$. The values of D were measured by AFM.
(c) Axial (*1*) and lateral (*2*) lengths of a voxel (an optical damage site) evaluated from optical microscopy (diffraction limit subtracted). Line *3* depicts a dependence $Length \propto Energy^2$. Curves are plotted to guide the eye.

lower than the detection limit in microscope observation, which is given by line*5* in Fig. 4(a). The fact that the damage fluence for $D = 0.1 - 0.4$ μm was slightly larger at $\lambda = 400$ nm than that at 800 nm can be explained by the established dependence for surface damage intensity $I_{damage} \propto 1/\sqrt{SpotArea}$.[28] This dependence describes, in fact, the importance of diffraction losses in the case of tight focusing into spot size with diameter close to λ. Recently, we reported similar LIDT dependence for an in-volume microstructuring of silica[29] found at tight focusing by $NA = 1.35$ objective lens, when the wavelength of fs pulses was changed from 400 nm to 800 nm.

We imaged the voxel (an optical damage site) in an optical microscope and the axial and lateral sizes were found not obeying eqn. 4 (Fig. 4(c)), as it was in the case of surface ablation (Fig. 4(a-b)). Instead, the axial length was found following $\propto Energy^2$ dependence for the voxels fabricated by an objective lens with $NA = 1.35$ till the cracking point marked by a boxed region in Fig. 4(c). The lateral size was not considerably changing with the pulse energy. Figure 4(c) shows data presented in the form comparable with the surface ablation given in Fig. 4(a-b). This observation can be explained by the focal intensity distribution of a Gaussian pulse, which decays laterally as $\exp(-radius)$, while axially as z^{-2}, where z is the distance from the focus. This eventually defines a focal region as a cylinder, what was observed experimentally examining voxels.

This shows that the spatial intensity distribution of the pulse are defining the feature sizes in both surface ablation and 3D microstructuring.

3.3. 3D fabrication by ablation: the "plasma spark" method

Here we introduce a new method of microstructuring of transparent solid materials by fs pulses. Fs-pulses are focused on the exit plane of the sample using plano-convex lens of focal length $f = 20-100$ mm. The amplitude of the electric field, E, on the exit plane is larger by a factor $2n/(n+1)$ as that on the entrance plane, here n is the refractive index of sample. If we disregard the absorption and reflection of the sample, which is low for transparent dielectrics in visible-to-near-infra-red spectral region, the enhancement up to 20% can be obtained for typical glasses (silica-based or polymers) with $n = 1.5$. The nature of enhancement is in the phase of reflected light, which undergo a phase shift of π for the entrance plane, since the light travels from the lower into the higher refractive index material. At the exit plane, there is no phase shift. This causes the total E-field at the entrance surface to be, usually, lower than that on the exit. When the intensity of ablation at the rear plane is reached, the ablation plume is visible (Fig. 5). The ablation front was scanned slowly, typically at 5-20 μm/s inside the sample. This fabrication could be called microstructuring by "plasma spark".

This method is different from microstructuring by self-focusing,[30] where the waist of the beam is at the entrance surface. Moreover, self-focusing would not allow to make microstructuring just a the surface, since a close presence

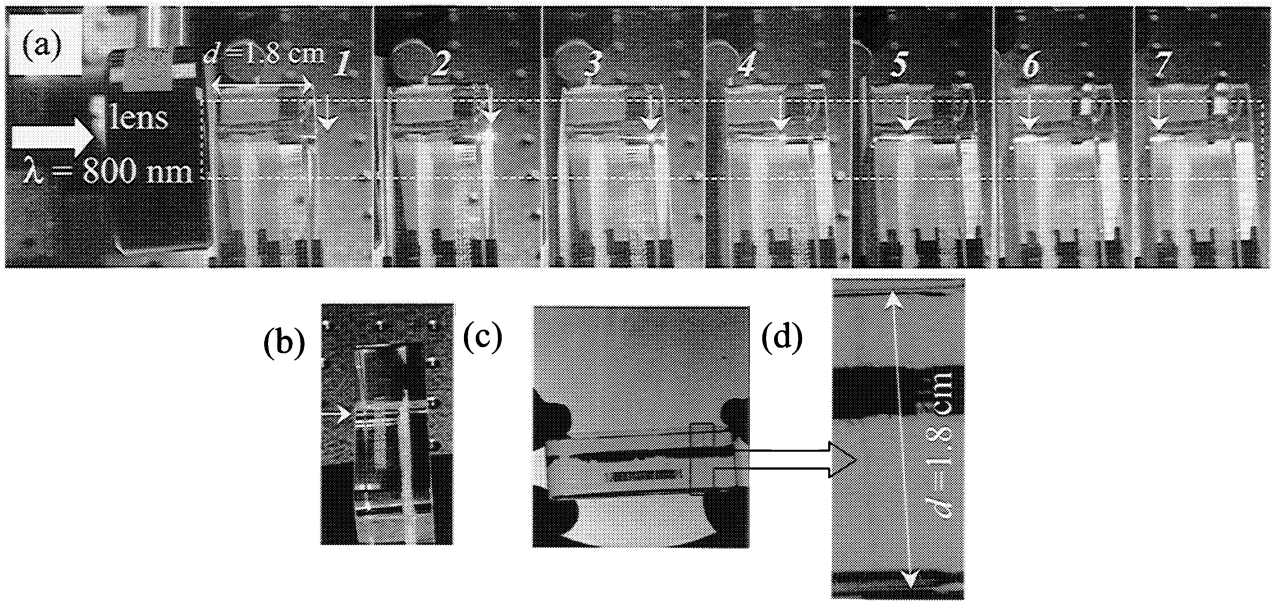

Figure 5. (a) Series of images (*1-7*) during "plasma spark" scanning throughout a 1.8 cm thick BK7 glass sample. Image *1* correspond to a focus location (pointed to by an arrow) just beneath the exit plane (a starting point for fabrication); *2* - at the exit and entrance planes, respectively. (b) Fabricated channel was imaged in the scattering light of introduced laser beam at 532 nm. (c) Image of the coloration of glass along the fabricated channel. (d) Close-up look at the coloration region of channel.

of the boundary disturbs the necessary conditions for self-focusing as we found in our experiments.

We applied this principle for a large-scale ($10^1 - 10^4$ μm) 3D microfabrication of borosilicate glass, technical grade of BK7. The fabrication of a channel was photographed and is shown in Fig. 5(a). Series $1 \rightarrow 7$ of images shows the translation of a "plasma spark", which location is pointed to by an arrow. The bluish light emission at $\simeq$ 365 nm observed to the left of an arrow (Fig. 5(a)) is caused by photoluminescence (PL) of L-centers, which defines an absorption edge of silicate glasses at 213 nm (5.8 eV).[31] This type of PL emission is only present for an intrinsic absorption of glass. Orange light seen to the right of arrows (Fig. 5(a)) is a signature of the light, caused by a "plasma spark", which was scattered on the walls of the just fabricated micro-channel. Similar results of microfabrication were obtained in the case of plastic acrylic glass.

An post-fabrication observation showed that a channel of $80 - 100$ μm in diameter was fabricated throughout almost 2 cm length of glass as shown in Fig. 5(b). Coloration of BK7 glass along the channel was clearly seen (Fig. 5(c-d)). This type of color center formation with absorption bands centered at 310 nm (4.0 eV), 440 nm (2.82 eV), and 640 nm (1.94 eV) is known to appear only at exposures to a light corresponding to the bandgap or shorter wavelengths absorption (including ionizing γ-/ and X-rays), also, to the absorption of high energy particles (electrons, neutrons, α-particles). These color centers can be annealed at $100 - 200$°C (a coloration disappears).

It was found that the optically damaged regions in borosilicate glass BK7 are etched much slower in BHF solution. This is, most probably, caused by the densification of glass around the channel. Even a presence of the defects, which had caused the coloration of glass, was not in favor of faster etching. However in pure silica, the etching contrast of optically damaged and fresh silica was such, that the 3D-channel fabrication was possible as we reported earlier.[32] The difference could be explained by the internal stress distribution around the damaged spots as presented in Fig. 6 by cross-polarized imaging along the channel. The stress was found highly localized around the channel in pure silica and was distributed much wider in the case of borosilicate glass. Further studies are planned to elucidate this mechanism.

Presence of densification under optical damaging with fs-pulses was also infered from Raman scattering data. To assess the structural modifications of silica the Raman spectrum was measured from a sample optically damaged by

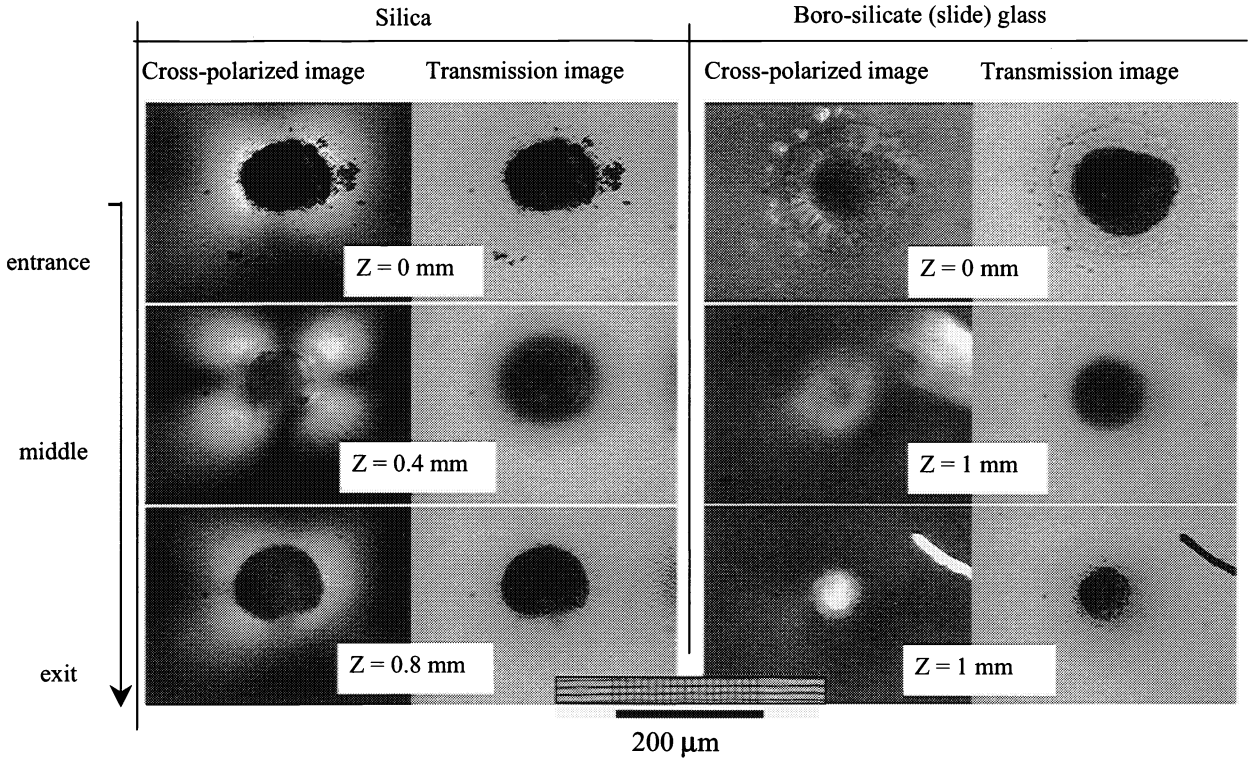

Figure 6. Cross-polarized and transmission images of optically damaged channels in silica (*Sumitomo*) and borosilicate slide glass (*Matsunami*). Focusing was made on the exit plane using a plano-convex lens with focal length of $f = 25$ mm. Then, the ablation plasma was transferred into the sample by translation along the beam propagation with approximate velocity of 0.2 mm/s. Laser power was 280 mW at 1 kHz repetition rate. The wavelength was 800 nm.

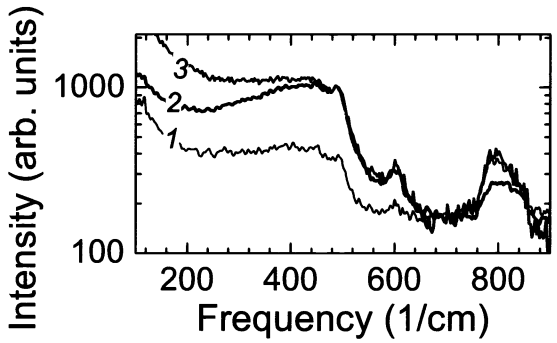

Figure 7. Raman spectra of silica before (*1* for VH and *2* for VV polarization) and after (*3* VH-pol.) optical damaging. Fluorescence background subtracted.

a single shot irradiation per voxel. Four layers of voxels with an average inter-voxel distance of 3 μm was recorded in a 150 μm-thick silica plate on the area of 4×4 mm^2. The spectra from damaged and fresh material are plotted in Fig. 7 (VV and VH denotes vertical-vertical and vertical-horizontal polarizations of illumination-detection setup, respectively). The band D_1 at 495 cm^{-1} is related to the regular puckered 4-ring structure vibrations and the D_2 band at 606 cm^{-1} is due to planar 3-ring vibrations, and 800 cm^{-1} band is due to collective, network, vibrations.[33] One can see, that the 4-ring structure vibrations have been decreased in intensity by a factor of 1.47 in comparison

with those of 3-membered rings, while the network vibrations were left almost unchanged. This points out that the bond breaking was taking place during optical damaging in favor of more dense 3-membered ring structures.

In the case of silica, the LIDT energy for 3D microstructuring was 24 nJ at a 50 μm depth. We can evaluate the corresponding total Si-O bond energy stored in the irradiated volume. Si-O bond energy is 432 kJ/mol and mass density of silica is 2.2 g/cm^2. The volume of focus can be approximated by the volume of cylinder, which height is twice the Rayleigh length, $2z_0$, and the radius of a base is the waist of the beam w_0. This gives the energy stored in Si-O bonding in the focal region to be 7.6 nJ. It means, when the chemical bonding energy comprises 29% of that in the light field, the LIDT is reached in silica. This is just a bit larger than the Lindeman melting criterion, x. For the most of materials $0.20 \leq x \leq 0.25$, what means that the melting starts when the time average deviation of an atom's position in respect to its equilibrium state comprises a value x of the interatomic distance.

4. CONCLUSIONS

We found that emission of $3/2\omega$ radiation was observed in silica at irradiation intensity higher than 1.6×10^{14}W/cm^2. Spectrally broad band emission observed at fluencies around optical breakdown can be qualitatively explained by classical *bremsstrahlung*. Large scale mm-to-cm 3D microstructuring of transparent materials can be achieved by using a novel, "plasma spark" method, which was successefully applied for microstructuring of silica, borosilicate, and acrylic glasses.

ACKNOWLEDGMENTS

This work was in part supported by the Satellite Venture Business Laboratory of the University of Tokushima. The authors are grateful for BK7 glass samples to Dr. O. Efimov. The discussions with Dr. A. Rode, Dr. M. Richardson and Dr. D. Ashkenasi are highly appreciated. We would like to acknowledge a collaboration with Dr. N. Novomlintsev for the Raman scattering measurements.

REFERENCES

1. M. Watanabe, H. Sun, S. Juodkazis, T. Takahashi, S. Matsuo, Y. Suzuki, J. Nishii, and H. Misawa, "Three-dimensional optical data storage in vitreous silica," *Jpn. J. Appl. Phys.* **37**(12B), pp. L1527–L1530, 1998.
2. M. Miwa, S. Juodkazis, T. Kawakami, S. Matsuo, and H. Misawa, "Femtosecond two-photon stereo-lithography," *Appl. Phys. A* **73**, pp. 561–566, 2001.
3. C. Quoix, G. Grillon, A. Antonetti, J.-P. Geindre, P. Audeberet, and J.-C. Gauthier, "Time-resolved studies of short pulse laser-produced plasmas in silicon dioxide near breakdown threshold," *Eur. Phys. J. AP* **5**, pp. 163–169, 1999.
4. S. Juodkazis, A. Marcinkevicius, M. Watanabe, V. Mizeikis, S. Matsuo, and H. Misawa, "Sub-picosecond optical damaging of silica: time resolved measurements of light induced damage threshold," in *Proc. SPIE vol. 4347, Laser-induced damage in optical materials: 2000*, G. J. Exarhos, A. H. Guenther, M. R. Kozlowski, K. L. Lewis, and M. J. Soileau, eds., pp. 212–222, 2001.
5. K. Yamasaki, S. Juodkazis, T. Lippert, M. Watanabe, S. Matsuo, and H. Misawa, "Dielectric breakdown of rubber materials by femtosecond irradiation," *Appl. Phys. A* , 2002. (In press).
6. R. R. Alfano and S. L. Shapiro, "Emission in the region 4000 to 7000 åvia four-photon coupling in glass," *Phys. Rev. Lett.* **24**, p. 584, 1970.
7. R. R. Alfano, *The Supercontinuum laser source*, Springer-Verlag, New York, (1989).
8. R. L. Fork, C. V. Shank, C. Hirlimann, R. Yen, and W. J. Tomlinson, "Femtosecond white-light continuum pulses," *Opt. Lett.* **8**, p. 1, 1983.
9. P. B. Corkum, C. Rolland, and T. Srinivasan-Rao, "Supercontinuum generation in gasses," *Phys.Rev. Lett.* **57**(18), pp. 2268–2271, 1986.
10. A. Brodeur, F. A. Ilkov, and S. L. Chin, "Beam filamentation and the white light continuum divergence," *Opt. Comm.* **129**, p. 193, 1996.
11. Q. Z. Wang, P. P. Ho, and R. R. Alfano *in ref. 6* , pp. 39–90.
12. Q. X. Li, T. Jimbo, P. P. Ho, and R. R. Alfano, "Temporal distribution of picosecond super-continuum generated in a liquid measured by a streak camera," *Appl. Opt.* **25**, p. 1869, 1986.
13. G. Y. Yang and Y. R. Shen, "Spectral broadening of ultrashort pulses in a nonlinear medium," *Opt. Lett.* **9**(11), p. 510, 1984.
14. N. Bloembergen, "Influence of electron plasma formation on superbroadening in light filaments," *Opt. Comm.* **8**(4), p. 285, 1973.
15. A. Penzkofer, "Parametrically generated spectra and optical breakdown in H_2O and NaCl," *Opt Comm.* **11**(3), p. 275, 1974.

16. F. A. Ilkov, L. S. Hkova, and S. L. Chin, "Supercontinuum generation versus optical-breakdown in CO_2 gas," *Opt. Lett.* **18**, p. 681, 1993.
17. Q. Feng, J. V. Moloney, A. C. Newell, E. M. Wright, K. Cook, P. K. Kennedy, D. X. Hammer, B. A. Rockwell, and C. R. Thompson, "Theory and simulation on the threshold of water breakdown induced by focused ultrashort laser pulses," *IEEE J. Quantum Electron.* **33**(2), p. 127, 1997.
18. H. Misawa, S. Juodkazis, S. Matsuo, V. Mizeikis, and A. Marcinkevicius, "Advantages and shortcomings of femtosecond laser microfabrication," in *Proc. 2002 Japan-USA Symp. on Flexible Automation*, 2002. (In press).
19. *Plasmas and Fluids*, Series: Physics through the 1990s, National Academy Press, Washington, D. C. Panel on the Physics of Plasmas and Fluids and Physics Survey Committee and Board on Physics and Astronomy and Commission on Physical Sciences, Mathematics, Resources and National Research Council, 1986.
20. A. A. Babin, A. M. Kiselev, K. I. Pravdenko, A. M. Sergeev, A. N. Stepanov, and E. A. Khazanov, "Experimental investigation of the influence of subterawatt femtosecond laser radiation on transparent insulators at axicon focusing," *Physics-Uspekhi* **42**(1), pp. 74–77, 1998.
21. E. G. Gamaly, A. V. Rode, V. T. Tikhonchuk, and B. Luther-Davies, "Ablation of solids by femtosecond lasers: ablation mechanism and ablation thresholds for metals and dielectrics," *Phys. Plasmas* , 2002. (In press).
22. I. H. Hutchinson, *Principles of Plasma Diagnostics*, Cambridge University Press, New York, 1987.
23. T. Kobayashi, T. Sekine, O. V. Fat'yanov, E. Takazawa, and Q. Y. Zhu, "Radiation temperatures of soda-lime glass in its shock-compressed liquid state," *J. Appl. Phys.* **83**(3), pp. 1711–1718, 1998.
24. Y. Kawaguchi, "Time-resolved fractoluminescence spectra of silica glass in a vacuum and nitrogen atmosphere," *Phys. Rev. B* **52**, pp. 9224–9228, 1995.
25. Y. Kawaguchi, "OH-content dependence of fractoluminescence spectra in silica glass," *Phys. Rev. B* **54**, pp. 9721–9725, 1996.
26. I. V. Ostrovskii, O. A. Korotchenko, T. Goto, and H. G. Grimmeiss, "Sonoluminescence and acoustically driven optical phenomena in solids and solid-gas interfaces," *Phys. Rep.* **311**(1), pp. 1–46, 1999.
27. X. Wang and X. Xu, "Thermoelastic wave induced by pulsed laser heating," *Appl. Phys. A* **73**, pp. 107–114, 2001.
28. W. Koechner, *Solid-state laser engineering*, Springer, Berlin, Heidelberg, 1999.
29. S. Juodkazis, M. Horiyama, M. Miwa, M. Watanabe, A. Marcinkevicius, V. Mizeikis, S. Matsuo, and H. Misawa, "Stereolithography and 3D microstructuring of transparent materials by femtosecond laser irradiation," in *Proc. SPIE of Int. Conf. on Laser and Laser Information Technologies (ILLA 2001), 23 - 25 June 2001, Vladmir, Russia.*, 2002. (In press).
30. D. Ashkenasi, H. Varel, A. Rosenfeld, S. Henz, J. Herrmann, and E. E. B. Cambell, "Application of self-focusing of ps laser pulses for three-dimensional microstructuring of transparent materials," *Appl. Phys. Lett.* **72**(12), pp. 1442–1444, 1998.
31. L. B. Glebov, "Optical absorption and ionization of silicate glasses," in *Proc. SPIE vol. 4347, Laser-induced damage in optical materials: 2000*, G. J. Exarhos, A. H. Guenther, M. R. Kozlowski, K. L. Lewis, and M. J. Soileau, eds., pp. 343–356, 2001.
32. A. Marcinkevicius, S. Juodkazis, M. Watanabe, M. Miwa, S. Matsuo, H. Misawa, and J. Nishii, "Femtosecond laser-assisted three-dimensional microfabrication in silica," *Opt. Lett.* **26**(5), pp. 277–279, 2001.
33. R. A. Barrio, F. L. Galeener, E. Martinez, and R. J. Elliott, "Regular ring dynamics in AX_2 tetrahedral glasses," *Phys. Rev. B* **48**(21), pp. 15672–15689, 1993.